



Design and implementation of miniaturized dual-mode terahertz bandpass filter based on swastik slotted fractals

S. Karthie¹ · V. Charan²

Received: 5 October 2024 / Accepted: 1 September 2025
© The Author(s), under exclusive licence to The Optical Society of India 2025

Abstract

This article presents the design of a miniaturized bandpass filter featuring a square patch perturbed microstrip resonator configuration with the Swastik fractal slots for applications in the terahertz regime. In the proposed design, the dual-mode behaviour of the filter is demonstrated with two transmission zeros on the passband edges, leading to a substantial improvement in selectivity. Besides, the presented terahertz filter, using a full-wave electromagnetic simulator, exhibits appreciable size reduction through the integration of Swastik fractal slots into the resonator, realizing miniaturization without compromising the desirable filter characteristics. Through proper optimization of the filter dimensions such as the perturbation and gap size, significant enhancements are also achieved in its return loss, insertion loss, and selectivity. The bandpass filter, measuring $8 \times 8 \mu\text{m}^2$, demonstrates notable performance at 3.88 THz with a return loss exceeding 38.32 dB and a low insertion loss of 1.63 dB. Furthermore, the presence of transmission zeros at 2.86 and 5.14 THz, on the left and right sides of the passband, indicates better suppression of out-of-band frequencies. The minimal footprint and better performance of the filter make it an ideal candidate for integration into the terahertz system, thereby enhancing the capabilities of terahertz-based communication and imaging technologies.

Keywords Microstrip patch resonator · Dual-mode bandpass filter · Fractal geometry · Swastik slots · Terahertz technology

Introduction

In the era of rapid advancements in communication technologies and the growing demand for high-speed data transmission, researchers have been driven to explore the realm of Terahertz technologies. The Terahertz frequency band, spanning from 0.1 to 10 THz, has become a focal point for experimentation and innovation. This underrated spectrum presents a vast array of opportunities for numerous

applications, including medical imaging, spectroscopy, and high-speed wireless communications. Terahertz imaging is a safe, non-ionizing, and non-invasive alternative to X-rays, penetrating non-metallic materials without causing damage, ideal for medical diagnosis, security screening, and scanning applications. This spectrum holds the promise of revolutionizing industries like medicine, security, and communication systems by enabling ultra-fast data transfer rates and scaling up next-generation networks. Although the Terahertz band offers immense potential, its implementation often faces challenges due to difficulties in the design and operation of components capable of functioning within this frequency range. Meanwhile, microwave engineering involves the design, analysis, and optimization of essential components that facilitate efficient signal transmission, reception, and processing. Key components include transmission lines, antennas, and filters, which are crucial for achieving precise control and transmission of microwave signals. Transmission lines guide waves with minimal loss, antennas transmit and receive waves, and filters select desired signals and

✉ S. Karthie
karthies@ssn.edu.in

V. Charan
charanvelavan12@gmail.com

¹ Department of Electronics and Communication Engineering, Sri Sivasubramaniya Nadar College of Engineering, Kalavakkam, Tamil Nadu 603110, India

² Department of Electronics and Communication Engineering, St. Joseph's College of Engineering, Chennai, Tamil Nadu 600119, India

reject unwanted frequencies for efficient processing and transmission.

Terahertz systems rely on bandpass filters to reduce interference and ensure signal clarity by selectively allowing specific frequency bands to pass. However, designing such filter structures requires innovative approaches to overcome material and structural limitations. Fractals, with their unique self-repeating and space-filling properties, have proven to be highly beneficial in designing multiband antenna structures for various wireless systems. The self-similarity of fractal geometry enables the miniaturization of filters and antennas, by allowing the repetition of patterns at smaller scales. This feature has led to the exploration of various fractal geometries in the design of bandpass filter, as researchers seek to harness their potential for improved performance and compactness. Notably, Sierpinski fractal curves [1] and Greek-cross fractal resonators [2] have been utilized to design compact bandpass filters with improved frequency responses and miniaturized microstrip structures. Dual-mode filter designs involving square-ring and cross-loop slots on traditional square [3] and octagonal [4] patch resonators have improved size compaction and frequency performance. Another design involving a novel loop resonator of star-shape [5] with a triangular perturbation achieves narrowband filtering, demonstrating a successful implementation of a compact dual-mode filter.

Researchers have designed various dual-mode bandpass filters with improved performances in which Cheng et al. [6] used a CSRR-perturbed square patch resonator, while others employed Koch fractal-based hexagonal loop resonators [7] or Moore fractal-based edge-coupled resonators [8], achieving benefits like reduced loss, compact size, and improved selectivity. Moreover, Neeboriya [9] and Song et al. [10] designed compact bandpass filters with improved performance in which the former fractal design uses an equilateral triangular resonator with low insertion loss and multiple transmission zeros, while the latter design employs a capacitive loading-based hexagonal loop resonator with better size reduction. Wu et al. [11] developed a dual-mode filter with slot-line stubs and slot patches on a square loop resonator, improving source-load coupling. Yeh et al. [12] demonstrated a diamond-structured filter model using a modified Minkowski fractal on a square patch resonator, enabling wideband responses and improved performance, including increased bandwidth and reduced loss.

Recently, there has been a growing interest in the research on terahertz filter designs, in addition to terahertz antennas, to unlock the full potential of terahertz technology and enable innovative applications across various disciplines. Notably, a spider-structured [13] and cross-slotted fractal [14] terahertz bandpass filters were designed through simulation, achieving transmittances of 100% and

70% respectively, across the terahertz range. Furthermore, a metamaterial-based design and fabrication of terahertz filter featuring cross-shaped structures [15] was demonstrated with 100% transmittance over a narrow bandwidth. Additionally, a waveguide bandpass filter structure with vanadium dioxide (VO_2) exhibiting a narrow bandwidth of 5 GHz and a transmittance of 98% was proposed for terahertz stealth applications [16].

The fabrication of another terahertz waveguide filter via micromechanical milling [17] was reported with a 3-dB bandwidth of 30 GHz, return loss of 15 dB, and a notable insertion loss of 3.9 dB, showcasing the potential of this manufacturing approach. A terahertz filter with a tunable centre frequency and bandwidth was designed utilizing split ring resonator grounded structures [18]. Furthermore, a quantitative study on the impact of diaphragm thickness on the performance of a low-loss terahertz waveguide bandpass filter [19] was conducted, revealing a significant correlation between diaphragm thickness and filter performance. Caroline et al. [20] developed a highly tunable terahertz bandpass filter using a metamaterial design that incorporates square and pentagonal CSRR structures, achieving 100% transmittance and making it an ideal candidate for applications in security screening and biomedical imaging. Researchers have made significant advancements in terahertz bandpass filters, including the exploration of plasmonic nanoparticle-enhanced CSRR-based filter at 1.5 THz by Yadollahzadeh and Baghban [21], the development of high-performance metamaterial-based multilayer filter with 93% transmittance by Asl et al. [22], and the design, fabrication, and verification of a cost-effective double-layer FSS-based filter at 0.9 THz with a flat passband, low insertion loss, and high band-edge steepness by Ri-Hui and Jiu-Sheng [23].

The Swastik fractal, inspired by the Swastika symbol, exhibits promising properties for filter design in signal processing. Its geometric characteristics, including self-similarity and symmetry, enable uniform frequency responses, essential in telecommunications and audio processing [24]. The integration of this ancient symbol into modern technology unveils the intersection of tradition and innovation, underscoring the value of interdisciplinary approaches [25]. The integration of Swastik-shaped slots in microstrip planar antennas enhances their performance for 5G applications, offering improved return loss, increased bandwidth, and optimized sub-6 GHz frequency operation. This results in the development of high-efficiency and high-gain antennas, making them suitable for next-generation wireless networks. The unique Swastik slot structure contributes substantially to these performance improvements, demonstrating the potential of fractal-based designs in modern communication systems. Furthermore, the recursive properties of fractals enable efficient computational algorithms, highlighting

their value in advanced antenna designs [26, 27]. These algorithms can be optimized for faster processing, which is essential for real-time applications such as streaming and live data analysis [28].

In general, a Swastika-shaped antenna patch is applied in advanced wireless communication systems, IoT devices, satellite communications, and wearable technology to enhance performance through improved bandwidth, compact design, multi-band capability, and optimized gain [29]. Besides, a simple miniaturized microstrip patch antenna, measuring $120 \times 120 \times 45 \mu\text{m}^3$, based on graphene was also designed and simulated for wideband terahertz applications [30]. Moreover, a comprehensive review of the current state and future potential of terahertz imaging and sensing technologies in healthcare applications, highlighting their emerging role and prospects for transforming medical imaging, diagnostics, and therapeutic interventions was presented by Gezimati and Singh [31]. As applications in terahertz spectrum continue to gain momentum, fuelled by increasing demand in areas like communications and imaging, it is crucial to develop technologies that strike a balance between high-quality implementation and cost-effectiveness, enabling sustained innovation and broader accessibility.

In this article, a miniaturized dual-mode bandpass filter based on Swastik slotted fractals is designed and implemented on a square patch resonator using CST Microwave Studio. Embedding a square perturbed element to the resonator along with orthogonal feedlines couples degenerate modes, generating two transmission zeros that improve selectivity and increase attenuation at the edges of passband. The proposed filter is a compact, simple, and high-performance solution, offering narrowband operation and excellent skirt selectivity. This innovative design is particularly significant because it operates in the terahertz range

of frequencies, which is emerging as a crucial spectrum for next-generation communication systems. The organization of this article begins by exploring the design and simulation of patch resonators (single and dual-mode configurations), followed by the evolution and simulation of Swastik slotted fractal structure geometry with its performance evaluation on *S*-parameters, gap size, perturbation size variations, and group delay, then comparing it to previous terahertz configurations, and finally ending with the conclusion.

Square patch resonator: single and dual-mode configurations

Figure 1 illustrates the topological geometry of square shaped patch resonator in single and dual-mode configurations. By utilizing RT/Duroid 6010 of high relative permittivity ($\epsilon_r = 10.7$) as the laminate, the design offers optimal performance for filter architecture. This design features a perfect electric conductor (PEC) for both the ground plane (0.5 μm thick) and patch, with the dual-mode functionality achieved by placing a perturbation of square shape at either a 45° or 135° angle relative to the 50 Ω feedlines, aligned with the diagonal symmetry (*D-D'*) plane of the square patch. This perturbation technique effectively induces dual-mode resonance, facilitating the design of a compact and efficient dual-mode filter. The dimensions of the patch are denoted by *A-A'* (horizontal) and *B-B'* (vertical), respectively. As the introduction of a perturbation along *D-D'* (diagonal) enables a dual-mode behaviour, the filter response is characterized by the presence of two transmission zeros. This dual-mode nature of the filter significantly enhances its selectivity, providing improved frequency rejection and reduced adjacent channel interference.

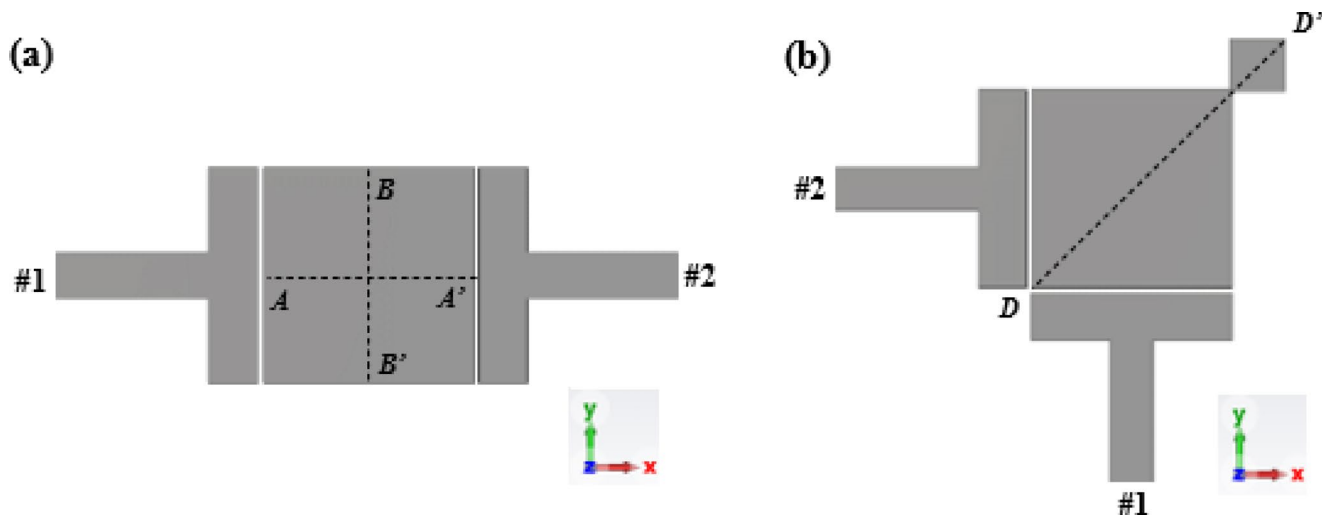


Fig. 1 Patch resonator geometry: **a** single and **b** dual-mode configurations having port assignments (Input #1; Output #2)

Figure 2 presents a comparative analysis of the simulated S-parameters for single and dual-mode resonator configurations. The single-mode nature of the resonator displays Chebyshev behaviour, resulting in inadequate selectivity for the bandpass filter, with a center frequency of approximately 4.34 THz. Conversely, the dual-mode nature of the resonator at 4.09 THz as seen in Fig. 2 offers quasi-elliptic behaviour with two distinct transmission zeros, yielding improved selectivity on both sides of the passband, for the perturbed dual-mode filter. This shows the efficacy of the perturbation technique in enhancing the filter selectivity.

Proposed swastik fractal slot-based dual-mode terahertz filter design

Figure 3 illustrates the proposed miniaturized dual-mode terahertz bandpass filter design, featuring the third iteration Swastik fractal slots, in both 3D visualization and top-view geometric layout. Without considering the feedlines, the size of the square resonator (L_r) in this design is set to $0.25\lambda_g$, in which the guided wavelength (λ_g) is calculated as 31.96 μm at 3.88 THz using Eq. (1) from Hong [32].

$$\lambda_g = \frac{c}{f_0 \times \sqrt{\epsilon_{refr}}} \quad (1)$$

The substrate and ground have identical square geometry, with a length (L_s) of 22 μm. Besides, the substrate and ground layers have their thickness maintained at 5 μm and 0.5 μm approximately. Excluding the perturbation patch along the diagonal, the square resonator has a patch thickness of 0.5 μm and a side-length (L_r) of 8 μm. The spacing between the resonator and the feedlines (g) is chosen to be 0.1 μm. The dimensions of the feedlines are 5.46 μm (L_1) × 1.60 μm (W_1), while the coupling arms at the input and output ports measure 8 μm (L_2) × 1.75 μm (W_2), respectively. Moreover, the resonator is split by a perturbation length (P) of 2 μm along its diagonal symmetry. The perturbation length with respect to the square patch resonator (L_p) is 1.91 μm. There are 3 iterations of the Swastik fractals, the distance between the first iteration of the Swastik fractal and the square patch resonator (D_0) is 3.9 μm. The physical dimensions of the designed terahertz bandpass filter after optimization are given in Table 1.

Fig. 2 S-parameter simulations for single and dual-mode patch resonator with transmission zeros at the passband edges enhancing filter performance

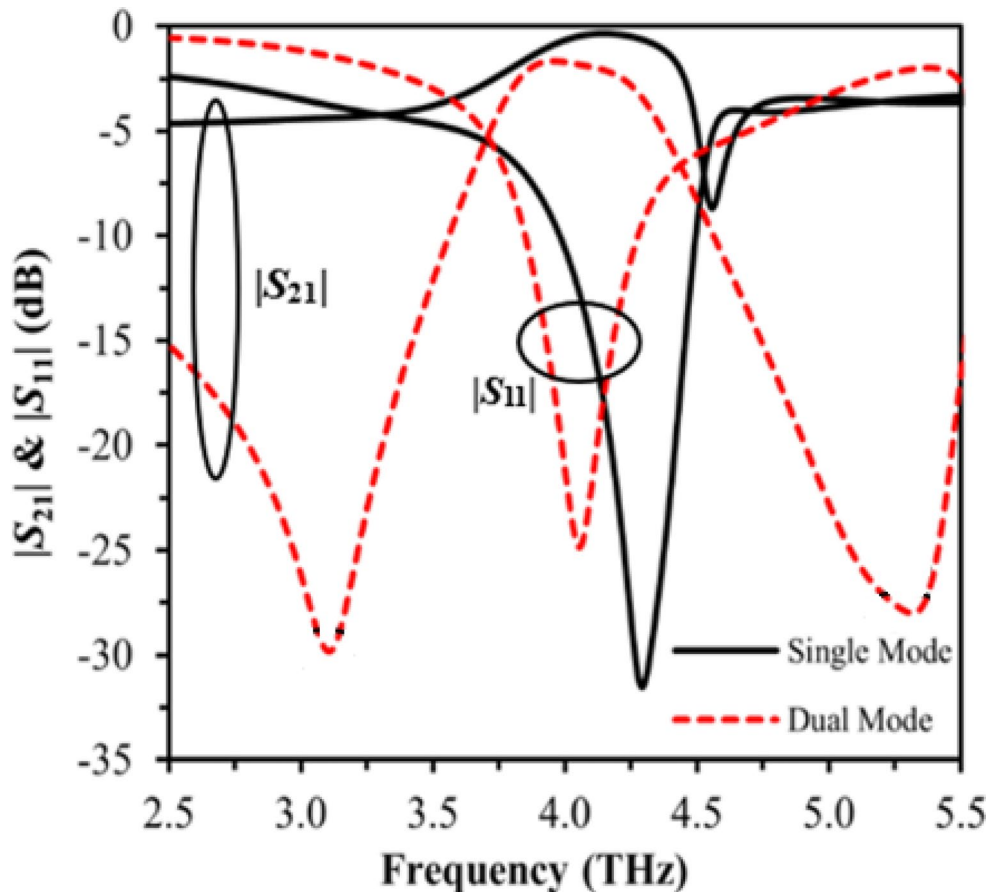


Fig. 3 Proposed miniaturized dual-mode Swastik slotted fractal bandpass filter design geometry: **a** 3D perspective-view of filter structure with substrate (5 μm thick) and metal plating (0.5 μm thick) layers and **b** top-view illustration of third iteration fractal structure

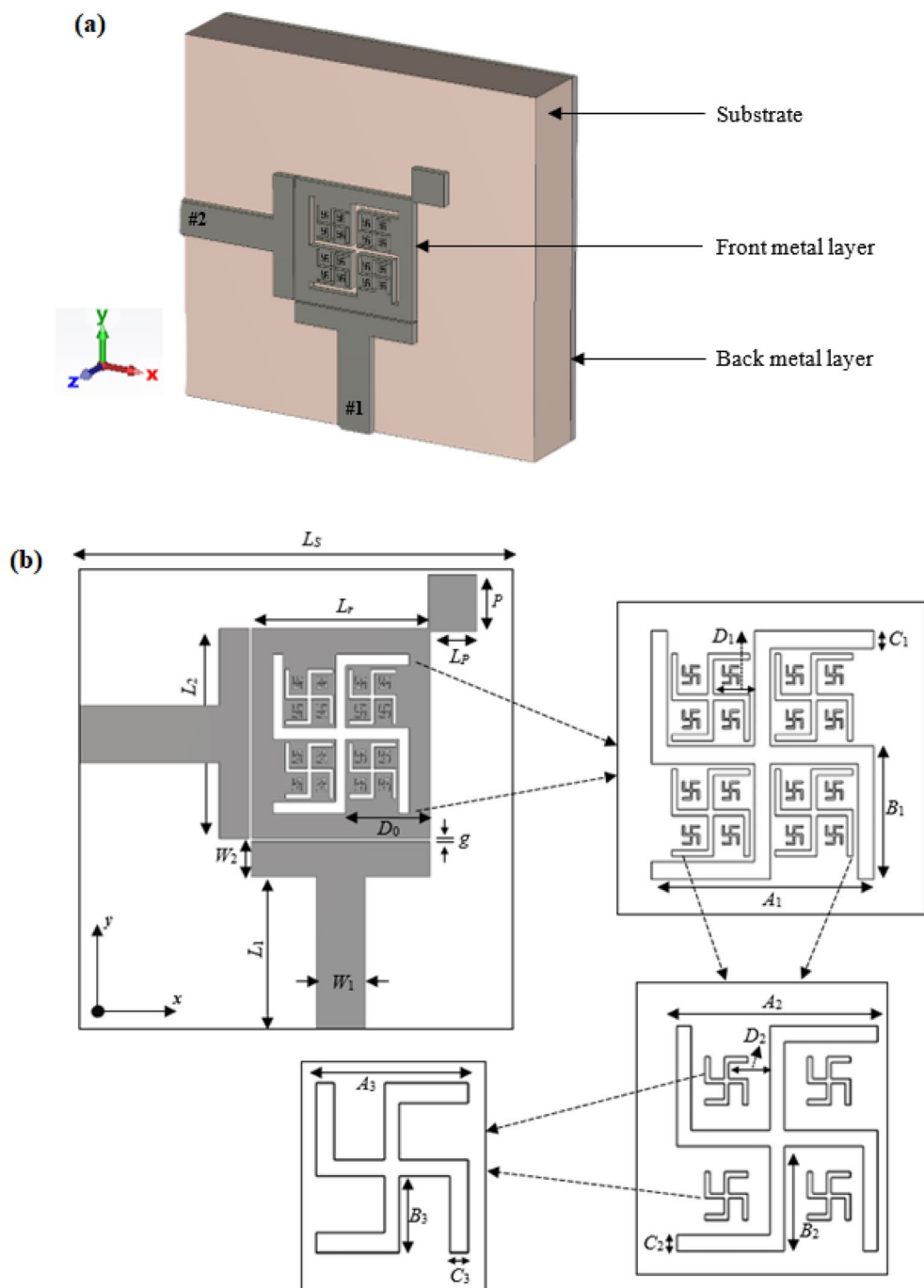


Table 1 Physical parameters and dimensions of the miniaturized filter

Substrate length, L_S (μm)	Resonator length, L_r (μm)	Feedline length, L_1 (μm)	Feedline width, W_1 (μm)	Coupling arm length, L_2 (μm)
22	8	5.46	1.60	8
Gap between square patch & coupling arm, g (μm)	Perturbation length, P (μm)	Perturbation length w.r.t square patch, L_p (μm)	Gap between square patch & first iteration, D_0 (μm)	Coupling arm width, W_2 (μm)
0.1	2.0	1.91	3.9	1.75

Development of swastik fractal slotted bandpass filter configuration

Figure 4 presents a series of iterations for the dual-mode bandpass filter structure, featuring Swastik fractal slots, highlighting its development. Figure 4a depicts the initial stage (zeroth iteration) of the resonator, where a square patch with a size of L_p , set to $0.25\lambda_g$, is presented. In the subsequent stage (Fig. 4b), a Swastik-shaped fractal, measuring 5.6 μm in length, 0.40 μm in width, and 2.60 μm in height,

Fig. 4 Evolution of Swastik slotted fractal structures in square perturbed patch resonator

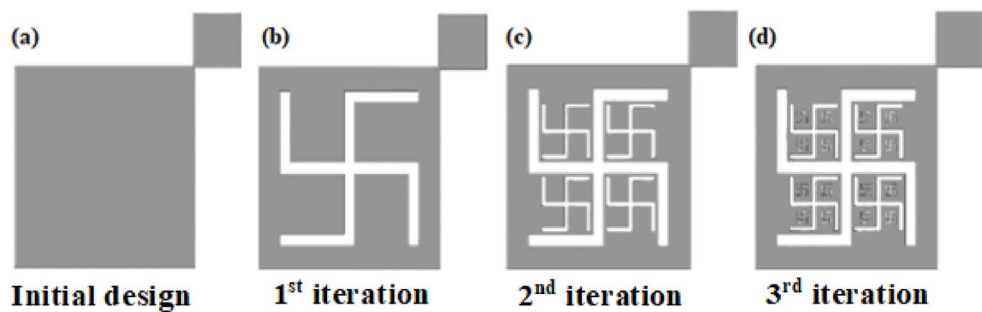


Table 2 Physical dimensions and parameters of swastik fractal slotted resonator (iteration 1 to 3)

Order of iteration, n	Length of Swastik fractal, A_n (μm)	Height of Swastik fractal, B_n (μm)	Width of Swastik fractal, C_n (μm)	Gap b/w n & $(n+1)$ th iteration, D_n (μm)
1	5.60	2.60	0.40	1.040
2	1.96	0.91	0.14	0.216
3	0.42	0.19	0.05	-

is centrally positioned on the resonator, and its impact is examined. Figure 4c shows the second iteration, where four smaller Swastik fractals ($1.96 \mu\text{m} \times 0.14 \mu\text{m} \times 0.91 \mu\text{m}$) surround the central Swastik fractal. In Fig. 4d, the third iteration is shown, where each space is filled with four smaller fractals ($0.42 \mu\text{m} \times 0.05 \mu\text{m} \times 0.19 \mu\text{m}$), resulting in sixteen additional fractals.

The dimensions of the Swastik fractals, from the longest to the smallest, are represented as A_1, A_2 , and A_3 for length; B_1, B_2 , and B_3 for width; and C_1, C_2 , and C_3 for height. The spacing between consecutive iterations are denoted as D_1 (between the first and second iterations) and D_2 (between the second and third iterations). The optimized dimensions of the Swastik fractals based on their iterations are summarized in Table 2.

S-parameter simulations of the presented terahertz bandpass filter design

The simulated performance of the dual-mode terahertz bandpass filter, illustrating the effects of fractal iteration and slotted structure integration on its frequency response is shown in Fig. 5. This figure compares the variation in return loss ($|S_{11}|$) and insertion loss ($|S_{21}|$) as the fractal design undergoes four iterations, highlighting the impact on filter performance. Here, $|S_{21}|$ is a measure of the transmission coefficient, which represents the ratio of the transmitted energy to the incident energy. A value close to 1 dB indicates minimal signal loss and high transmission efficiency. $|S_{11}|$ is a measure of the reflection coefficient, which represents the ratio of the reflected energy to the incident energy, ideally approaching infinity. However, in practical

applications, $|S_{11}|$ value greater than 10 dB is generally considered acceptable, indicating a minimal amount of signal reflection. Figure 5 clearly shows the center frequency decreases significantly from iteration 0 (square patch) to iteration 1 (Swastik fractal), with further iterations showing a continued, albeit smaller, decrease.

The presented filter design exhibits peak resonant frequencies of 4.19 THz for the initial square patch, decreasing to 3.909 THz with the addition of the large Swastik fractal, further reducing to 3.891 THz with four smaller Swastik fractals, and ultimately reaching 3.8812 THz with the inclusion of sixteen smaller Swastik fractals alongside the long and small Swastik fractals. By incorporating slots into the design, the signal path is extended, which increases the resonator's internal inductance and consequently reduces the resonant frequency due to the enhanced inductive effect. As a result, the reduced resonant frequency facilitates a more compact circuit design, contributing to the miniaturization of the overall filter structure. This beneficial characteristic of the resonator plays a crucial role in achieving a compact dual-mode bandpass filter design. As the resonant frequency drops from 4.19 THz to 3.88 THz, the patch size correspondingly shrinks by as much as 25.93%, achieving a more compact design. The design also features two prominent transmission zeros with high rejection levels of approximately 33.10 dB and 24.63 dB, located at 2.85 THz and 5.14 THz, respectively. These transmission zero frequencies significantly enhance the selectivity by providing steep roll-offs on passband edges of the filter. This design leverages the quasi-elliptic characteristics of these transmission zeros, resulting in enhanced performance and a more efficient filtering response. The downward shift in resonant frequency is also observed in the $|S_{11}|$ characteristics as the signal path lengthens with the introduction of slots. Meanwhile, Table 3 provides a comprehensive comparison of the simulated responses for the filter across fractal iterations 0 to 3 including the proposed design with multiple Swastik slotted fractals.

Fig. 5 Comparative analysis of S -parameters for dual-mode terahertz filter designs: Conventional square patch (iteration 0) vs. Swastik fractal slotted structures (iterations 1–3)

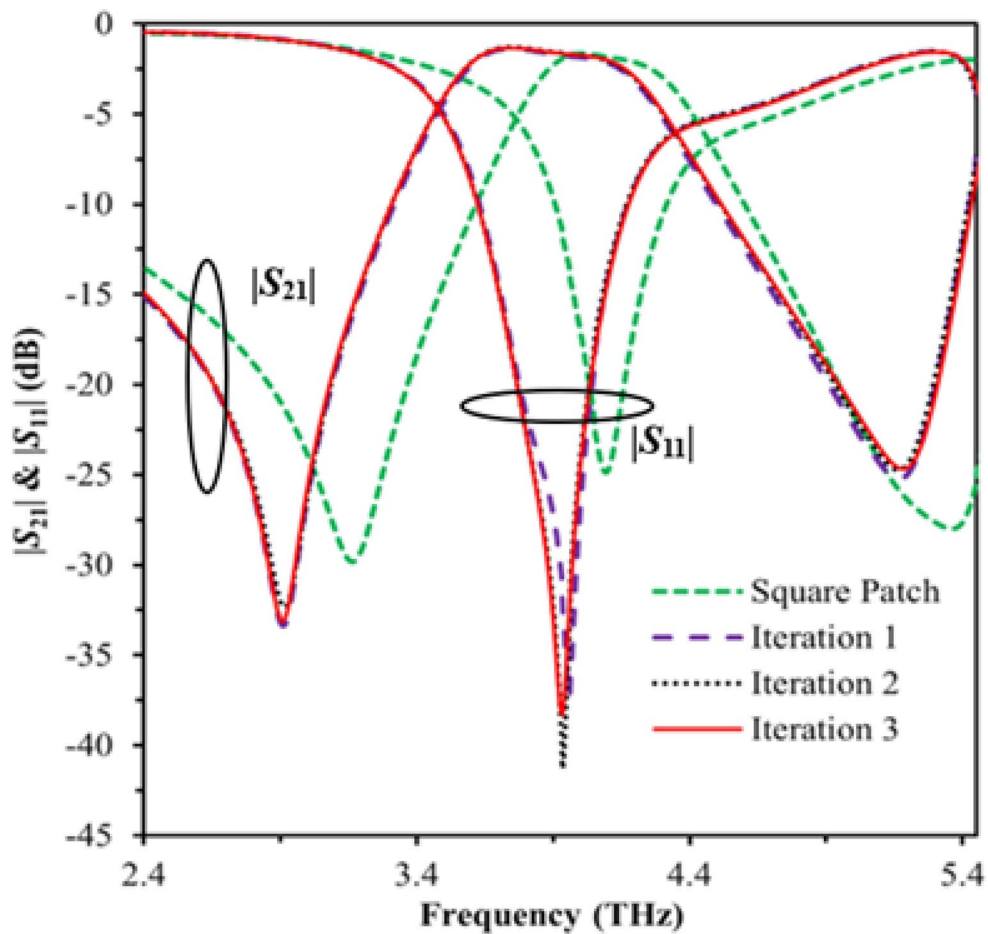


Table 3 Simulated characteristics of the swastik slotted fractal resonator structure

Performance parameters of resonator	Initial design (iteration 0)	First iteration	Second iteration	Third iteration
f_0 (THz)	4.095	3.909	3.891	3.8812
3-dB bandwidth (GHz)	659	787	799	788
Fractional bandwidth (%)	16.09	20.13	20.53	20.30
Rejection level (dB) at transmission zero frequencies (THz)	30.26 @ 3.12, 27.97 @ 5.31	33.33 @ 2.877, 25.17 @ 5.13	32.21 @ 2.874, 24.74 @ 5.12	33.10 @ 2.856, 24.63 @ 5.14
Insertion loss (dB)	1.72	1.787	1.660	1.637
Return loss (dB)	24.87	37.138	40.952	38.326
Reduction in frequency (%)	0	4.425	4.951	5.221
Reduction in patch size (%)	0	15.86	23.63	25.93

Evaluation of Terahertz filter performance

The design of the presented terahertz dual-mode bandpass filter is realized through the careful optimization of gap size and perturbation size, and its performance is then subsequently analyzed. Additionally, the research examines the impact of perturbation size on the filter's mode-splitting behaviour, highlighting the importance of perturbation in achieving desired dual-mode characteristics.

The effect of gap size (g) variation between the patch resonator and coupling arms on the frequency response of the filter is examined, with g ranging from 0.1 to 0.4 μm . Figure 6 illustrates that decreasing g results in a slight reduction in insertion loss, approximately 0.5 dB. This suggests that gap size optimization can lead to improved filter performance, but with limited potential for substantial enhancement. In addition, the left transmission zero shifts downward notably, while the upper transmission zero exhibits a slight shift as g varies. Regardless of the gap size variation, the return loss remains consistently high, exceeding 9.5 dB. As evident from Fig. 6, a gap size of $g=0.1 \mu\text{m}$ yields optimal results for both $|S_{21}|$ and $|S_{11}|$ parameters, outperforming other gap sizes. This indicates that a gap size of 0.1 μm is

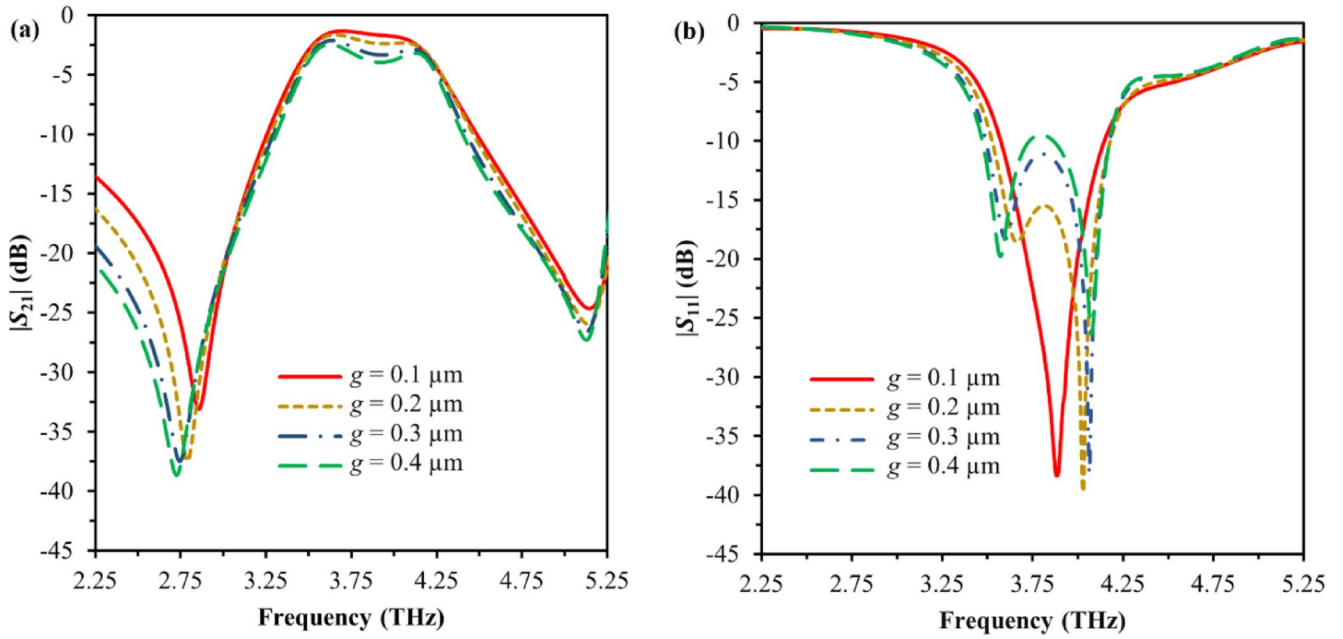


Fig. 6 Impact of gap size (g) variation on final iteration structure: **a** $|S_{21}|$ and **b** $|S_{11}|$. for g values ranging from 0.1 to 0.4 μm

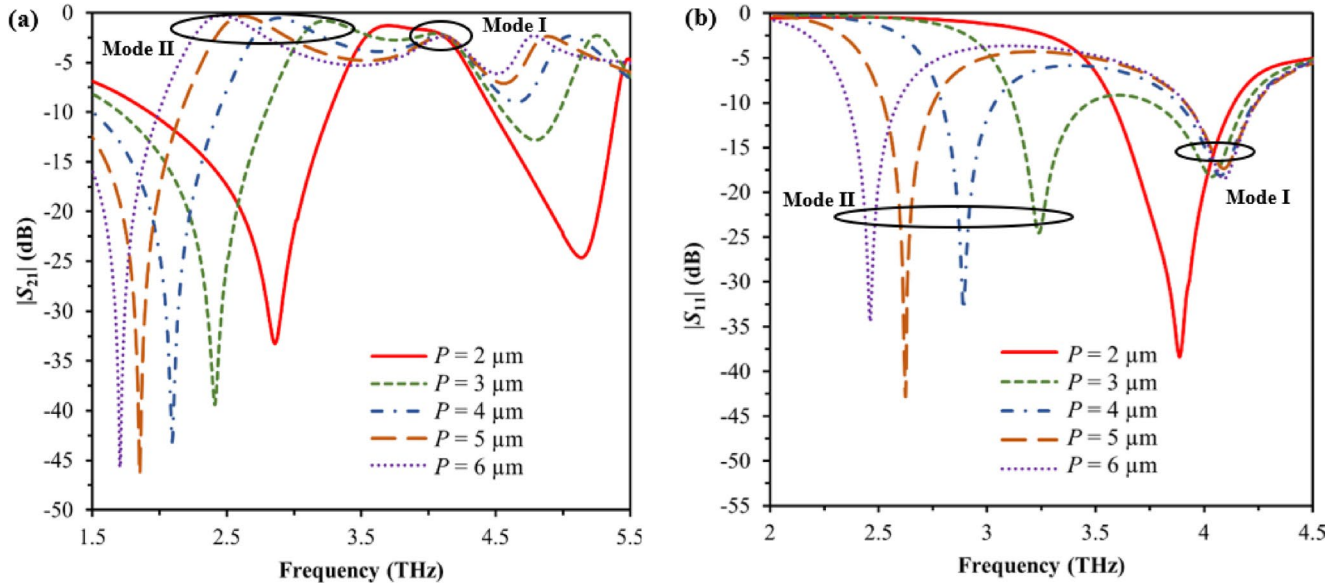


Fig. 7 Impact of perturbation size (P) variation on final iteration structure: **a** $|S_{21}|$ and **b** $|S_{11}|$. for P values ranging from 2 to 6 μm

the optimal choice for achieving good filter performance, balancing both insertion loss and return loss.

Figure 7 illustrates the $|S_{21}|$ and $|S_{11}|$ characteristics of the filter for variation in its perturbation size (P). In the $|S_{21}|$ response of Fig. 7a, it is noticed that the upper transmission zero experiences a relatively minor shift to higher frequencies, in contrast to the lower transmission zero, which exhibits a more substantial shift to lower frequencies. Here, the transmission zeros exhibit sharp transitions at $P=2 \mu\text{m}$. However, as P increases, the upper transmission zero becomes progressively broader, with a corresponding

decrease in its $|S_{21}|$ value. As P increases from 2 to 6 μm , there is emergence of two degenerate modes, denoted as mode I and mode II, and the resonant frequency shift of mode I is less pronounced compared to that of mode II. Similarly, Fig. 7b illustrates a corresponding effect in the filter's $|S_{11}|$ response, where two poles emerge in the passband as P increases from 2 to 6 μm . The upper poles experience a minor shift to higher frequencies, while the lower poles exhibit a more substantial shift to lower frequencies. Notably, better filter performance is attained at $P=2 \mu\text{m}$,

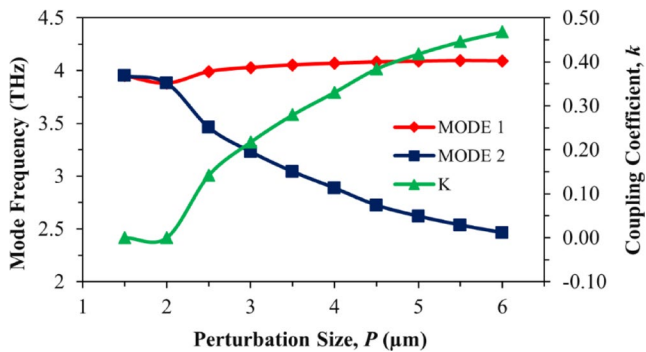


Fig. 8 Dual-mode splitting behaviour as a function of perturbation size (for P values ranging from 2 to 6 μm)

emphasizing the critical role of perturbation size optimization in achieving optimal filter response.

The impact of perturbation size (P) on the split characteristics of the dual-mode terahertz bandpass filter is illustrated in Fig. 8. The split in resonant frequencies into two modes as mode I and mode II are evident from Fig. 8, as P increases from 2 μm , exhibiting significant frequency variations that lead to an expansion of the bandwidth and a consequent reduction in selectivity of the filter. As also seen from Fig. 8, there is an increase in the coefficient of coupling (k) between the two modes, which is calculated using (2)

$$k = \frac{f_{01}^2 - f_{02}^2}{f_{01}^2 + f_{02}^2} \quad (2)$$

where f_{01} and f_{02} represents the center frequencies of mode I and II, respectively, highlighting the dependence of modal coupling on perturbation size. When the perturbation size is 2 μm or less, the filter displays single-mode behaviour, resulting in a negligible coupling coefficient ($k \approx 0$).

Results and discussion

The simulated performance of the miniaturized terahertz bandpass filter is obtained using the optimized structural dimensions of the resonator and the Swastik slotted fractals of third iteration. The simulated group delay characteristics, shown in Fig. 9, indicate a group delay of 0.8 ps in time-domain for the designed terahertz filter, with minimal variation in the passband. This suggests that the filter demonstrates excellent linearity in transmitting the desired signals, with the output signal being a faithful replica of the input signal, delayed by a consistent 0.8 ps.

To achieve a dual-mode frequency response characteristics, shown in Fig. 10, the optimized filter structure is utilized and it exhibits favourable performance at 3.88 THz, with a low insertion loss of 1.63 dB, a high return loss of 38.326 dB, and significant rejection levels of 33.10 dB and 24.63 dB at the well-defined transmission zero frequencies of 2.86 and 5.14 THz, in the lower and upper passband edges. In addition, the filter boasts a 3-dB narrow bandwidth of 0.788 THz, highlighting its ability to selectively transmit frequencies within this range.

Figure 11 illustrates the current distribution along the surface of the terahertz filter, providing insight into the spatial arrangement of current flow and electromagnetic field intensity across the filter's surface. At frequencies corresponding to the transmission zeros (2.86 THz and 5.14 THz), substantial signal attenuation (i.e., $|S_{21}| = 33.10$ dB and 24.63 dB) occurs, which is shown by the dark blue colouration in Fig. 11a and c, indicating minimal power transfer (low current distribution) to the output port. Conversely, the attenuation is minimum (i.e., $|S_{21}| = 1.63$ dB) at the resonant frequency (3.88 THz), allowing maximal energy transfer (high current distribution) to the output port, represented by the red-amber hue in Fig. 11b.

The simulated optical spectra in Fig. 12 reveal the reflectance, absorbance, and transmittance characteristics of the presented filter configuration in dual-mode. The filter achieves a transmittance of 0.705, with no reflectance and an absorbance of 0.313 at resonance (3.88 THz). Moreover,

Fig. 9 Group delay characteristics of 3rd iteration terahertz filter exhibiting excellent linearity in the passband with a flat response of 0.8 ps

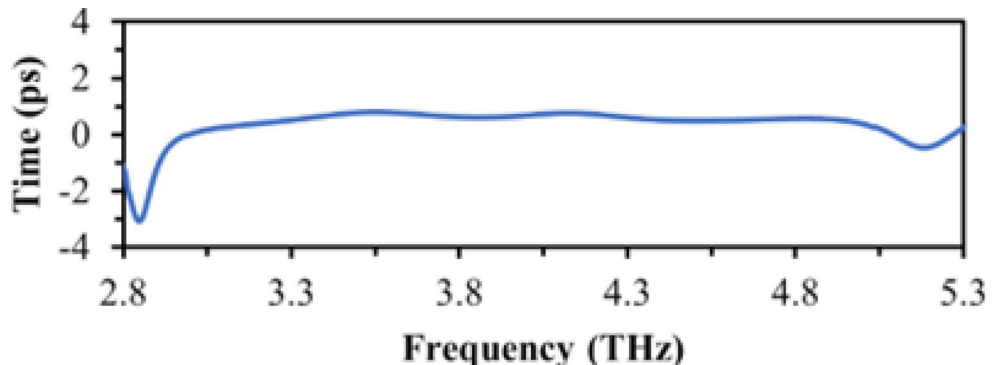


Fig. 10 Dual-mode filter response at 3rd iteration of Swastik fractals: S -parameter characteristics with sharp transmission zeros at 2.86 THz and 5.14 THz

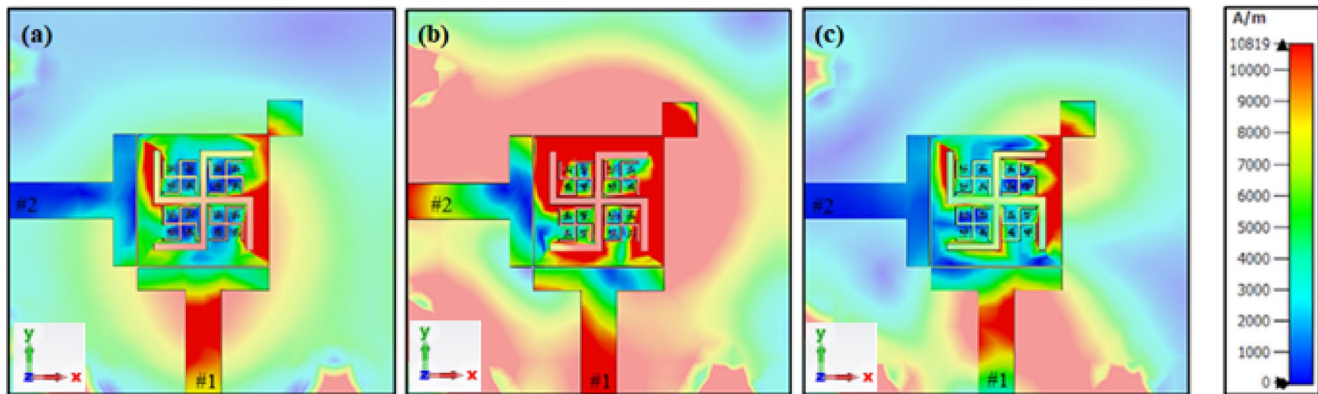
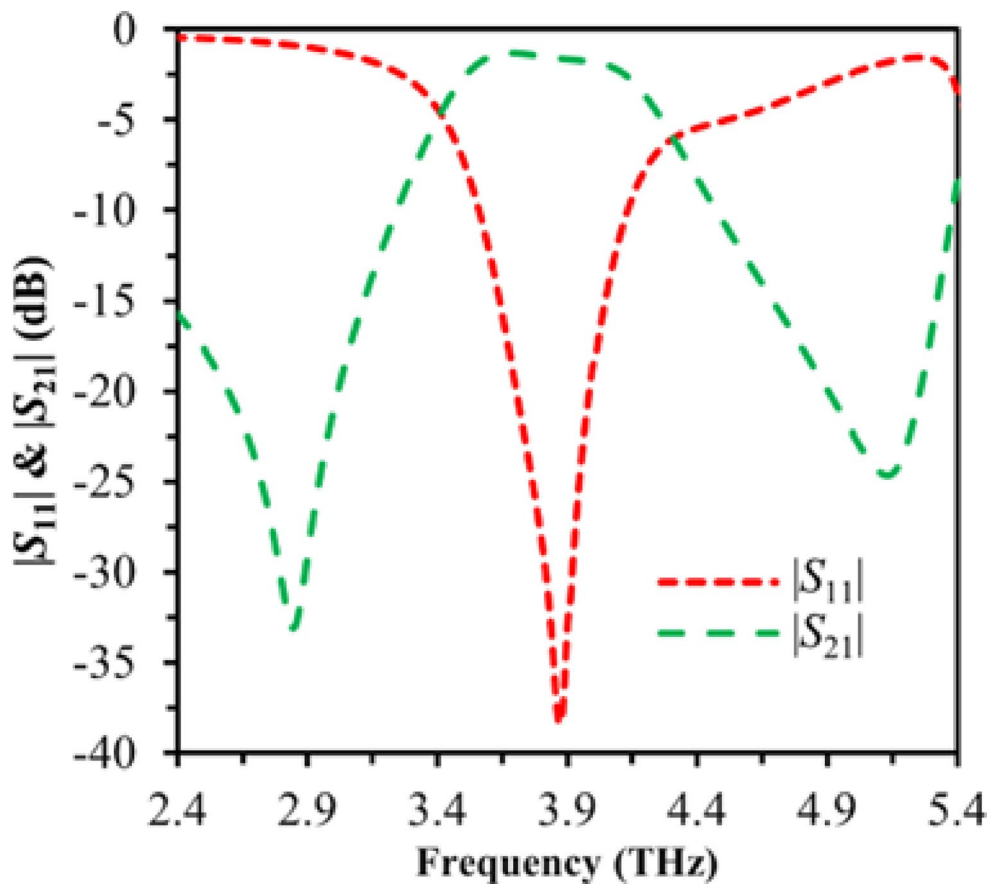


Fig. 11 Visualizing surface current distribution on Swastik fractal resonator: Frequency-dependent patterns at **a** 2.86 THz, **b** 3.88 THz, and **c** 5.14 THz. Intensity gradient: Red (Highest) to Dark Blue (Lowest)

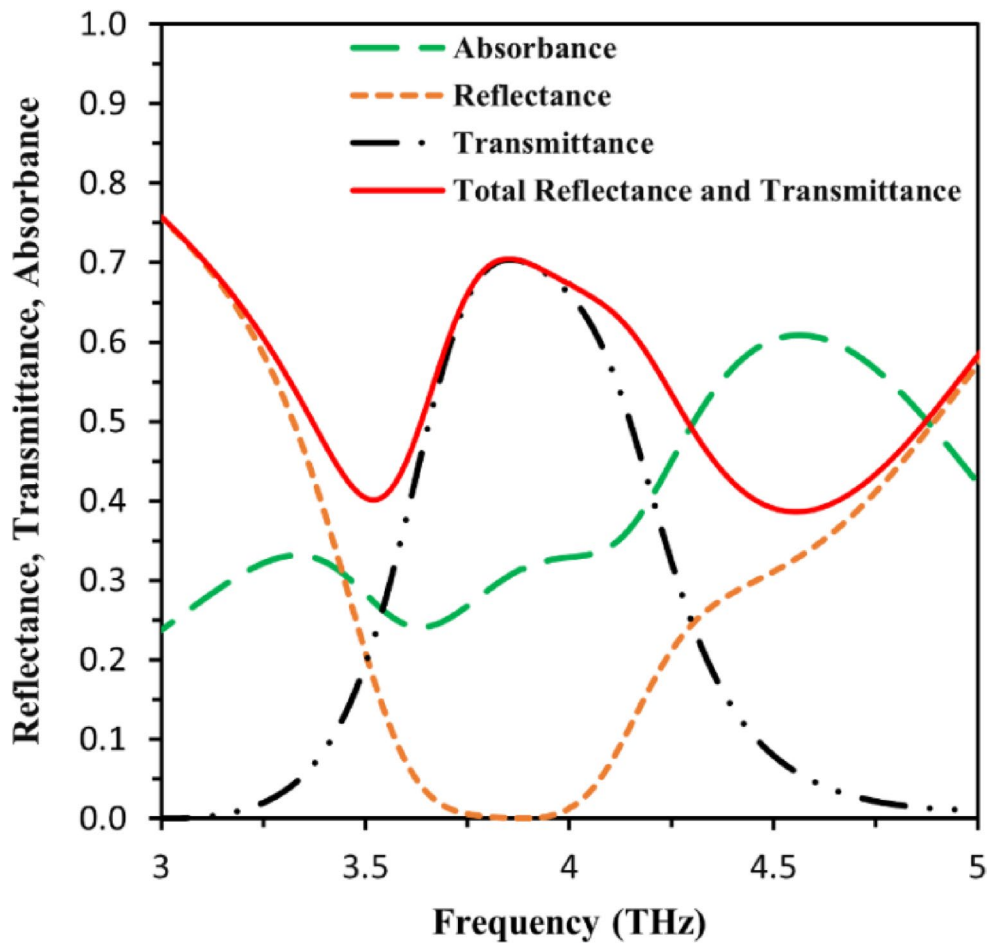
the filter provides a narrow bandwidth (0.788 THz) and its transmittance profile displays a clear bandpass filter characteristics in the passband, highlighting the selective frequency transmission capabilities of the filter.

Figure 13 presents the spectral characteristics of the terahertz fractal filter designed in this study, simulated over a wide frequency range from 0 to 15 THz. At a resonance of 3.88 THz, the results reveal a peak transmittance of approximately 70%, indicating optimal filter performance.

Additionally, the emergence of smaller resonances at frequencies beyond the center frequency, with transmittance values below 55%, demonstrates the filter's ability to effectively reject signals outside the passband, while achieving sufficient transmittance at resonance, thereby confirming the high selectivity and spectral purity of the filter.

Table 4 provides a comparative analysis of the presented filter with existing terahertz bandpass filter designs, including notable implementations based on VO₂ [16], PTFE

Fig. 12 Simulated optical properties of the 3rd iteration terahertz bandpass filter: absorbance, reflectance, and transmittance spectra



[20], SiO₂ [22], Al nanoparticles [21], and waveguide structures [17, 19], as well as the hexagonal lattice array filter design with circular holes [23]. In contrast, the presented work featuring Swastik fractal structures stands out due to its simplicity, dual-mode planar filter architecture, and cost-effective design on RT/Duroid substrate, making it a promising solution for applications in terahertz field where cost and complexity are critical factors.

Moreover, it outperforms the reported designs by offering an impressive return loss of 38.3 dB, a low group delay of 0.8 ps, and a compact footprint of $8 \times 8 \mu\text{m}^2$, although it has a relatively low transmittance of 70%. While the PTFE-based filter [20] exhibits superior performance metrics, its larger physical footprint ($14 \times 14 \mu\text{m}^2$) and an increased group delay of 3670 ps are notable drawbacks, as compared with this design, which imparts a balanced combination of compactness and performance. Although VO₂-based filter [16] at 1.164 THz achieves a high transmittance of 98% and a narrow bandwidth of 5 GHz, its size is comparatively large, and additionally, other key filter performance metrics are not provided in the report. Besides the current design, only a limited number of studies [17, 19, 20] have reported on key filter performance metrics such as return loss and

insertion loss in terahertz regime. Compared to their gigahertz counterparts, terahertz filters boast faster data transfer rates, enhanced quality of service, reduced footprint, and greater miniaturization capabilities, rendering them an appealing choice for cutting-edge applications.

Conclusion

In this study, a miniaturized bandpass filter utilizing the Swastik fractal slots on the resonator is proposed and designed at 3.88 THz. The presented filter design leverages the square perturbed resonator with perpendicular feed ports for proper excitation and coupling of the dual degenerate modes, yielding a dual-mode nature. This fractal slotted design approach facilitates the realization of a compact filter with a reduced size of $8 \times 8 \times 6 \mu\text{m}^3$, making it an attractive solution for integrated terahertz systems. Significant reduction in frequency (5.22%) and patch size (25.93%) are observed for the proposed filter with fractal slots over the traditional patch resonator, resulting in miniaturization. Additionally, the filter demonstrates excellent frequency selectivity, with two transmission zeros located at 2.86 THz

Fig. 13 Terahertz bandpass filter spectral performance: Wideband response with a maximum transmittance of 70% at 3.88 THz

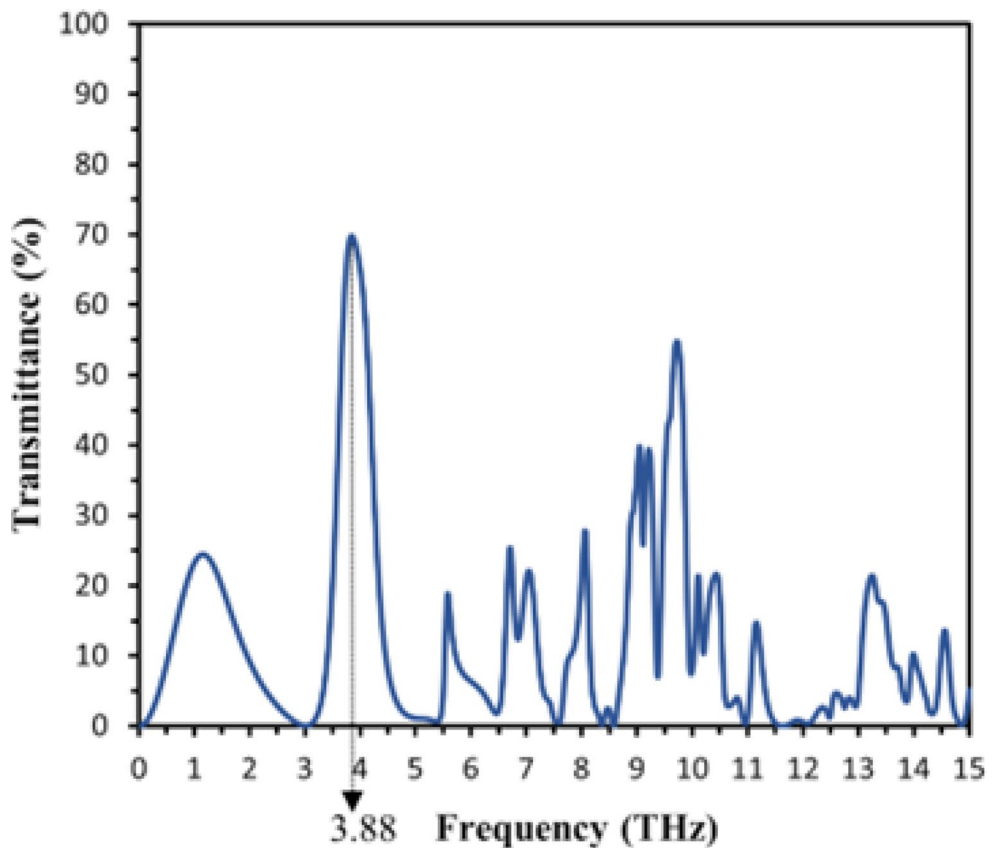


Table 4 Comparative analysis of the proposed Terahertz bandpass filter with previous research

Parameters	This work	[16]	[17]	[19]	[20]	[21]	[22]	[23]
Material used	RT/Duroid 6010 laminate	VO ₂	WR-2.2 wave guide	WR-2.8 wave guide	PTFE	Al nano particles	SiO ₂	Tin foil
f_0 (THz)	3.88	1.164	0.255	0.340	7.0	1.5	1–3	0.90
3-dB bandwidth (THz)	0.788	0.005	0.030	0.018	1.6	1	1	0.20
Fractional bandwidth (%)	20.3	0.43	11.76	5.3	22.85	66.67	33.33	22
$ S_{21} $ (dB)	1.63	NA	3.9	0.6	0.001	NA	NA	0.7
$ S_{11} $ (dB)	38.3	NA	15	20	28.66	NA	NA	NA
Transmittance (%)	70	98	NA	NA	100	90	93	97
Group delay (ps)	0.8	NA	NA	NA	3670	NA	NA	NA
Size (μm^2)	8×8	560×560	560×280	2120×1820	14×14	72×72	52.8×52.8	$20,000 \times 20,000$

and 5.14 THz, providing 33.10 dB and 24.63 dB suppression levels on the passband edges, respectively. Furthermore, the filter achieves a narrow 3-dB bandwidth of 0.788 THz and a fractional bandwidth of 20.3% within the passband, indicating high selectivity. The designed filter showcases good performance metrics, including a return loss exceeding 38.3 dB and an insertion loss below 1.63 dB, making it a viable candidate for terahertz frequency range applications demanding high-performance filtering capabilities.

Author contributions All authors contributed equally to this work.

Funding No funding was received by the authors for conducting this study.

Declarations

Conflict of interest The authors declare no conflict of interest.

Compliance with ethical standards This article does not contain any studies with human participants or animals performed by any of the authors.

References

- Y.S. Mezaal, H.T. Eyyuboglu, J.K. Ali, New dual band dual-mode microstrip patch bandpass filter designs based on Sierpinski fractal geometry. In *IEEE International Conference on Advanced*

- Computing and Communication Technologies.* 348–352 (2013). <https://doi.org/10.1109/ACCT.2013.55>
2. H. Lu, W. Wu, J. Huang, X. Zhang, N. Yuan, Compact dual-mode microstrip bandpass filter based on Greek-cross fractal resonator. *Radioengineering.* **26**(1), 275–284 (2017). <https://doi.org/10.13164/re.2017.0275>
 3. S. Karthie, J. Zuvairiya Parveen, D. Yogeshwari, E. Venkadeswari, Compact dual-mode microstrip bandpass filter based on slotted square patch resonator. *Microelectron. Int.* **39**(2), 49–57 (2022). <https://doi.org/10.1108/MI-08-2021-0080>
 4. S. Karthie, S. Salivahanan, Fractally slotted patch resonator-based compact dual-mode microstrip bandpass filter for wireless LAN applications. *AEU Int. J. Electron. Commun.* **107**, 264–274 (2019). <https://doi.org/10.1016/j.aeue.2019.05.037>
 5. K.G. Avinash, I.S. Rao, Compact dual-mode microstrip bandpass filters with transmission zeros using modified star-shaped resonator. *Prog Electromagn. Res. C* **71**, 177–187 (2017). <https://doi.org/10.2528/PIERC16122801>
 6. Y. Cheng, C. Mei, L. Zhu, Design of dual-mode band-pass filter with novel perturbation elements. *Prog Electromagn. Res. C* **96**, 59–71 (2019). <https://doi.org/10.2528/PIERC19061708>
 7. S. Neethu, S. Santhosh Kumar, Microstrip bandpass filter using fractal based hexagonal loop resonator. In *IEEE International Conference on Advances in Computing and Communications.* 319–322 (2014). <https://doi.org/10.1109/ICACC.2014.81>
 8. Y.S. Mezaal, J.K. Ali, H.T. Eyyuboglu, Miniaturised microstrip bandpass filters based on Moore fractal geometry. *Int. J. Electron.* **102**(8), 1306–1319 (2015). <https://doi.org/10.1080/00207217.2014.971351>
 9. S. Neeboriya, Novel dual-mode microstrip triangular patch resonator bandpass filter. *J. Commun. Technol. Electron.* **64**, 1445–1449 (2019). <https://doi.org/10.1134/S106422691912012X>
 10. K. Song, Y. Zhu, M. Zhao, M. Fan, Y. Fan, Miniaturized bandpass filter using dual-mode hexagonal loop resonator. *Int. J. Microw. Wirel. Technol.* **9**(5), 1003–1008 (2017). <https://doi.org/10.1017/S1759078716001094>
 11. B. Wu, W. Su, S.J. Sun, C.H. Liang, Novel dual-mode bandpass filter using slot-line square loop resonator. In *IEEE International Conference on Microwave and Millimeter Wave Technology.* 1–3 (2012). <https://doi.org/10.1109/ICMWT.2012.6230056>
 12. K.D. Yeh, H.H. Liu, J.C. Liu, An equivalent circuit model for the wide-band band-pass filter with the modified Minkowski-island-based fractal patch. *Int. J. RF Microw. Comput. Aided Eng.* **24**(2), 170–176 (2014). <https://doi.org/10.1002/mmce.20745>
 13. H. Shahounvand, A. Fard, Design and simulation of a new narrow terahertz bandpass filter. *SN Appl. Sci.* **2**, 1814 (2020). <https://doi.org/10.1007/s42452-020-03514-3>
 14. S. Karthie, K. Raksha Madhuri, G. Varshini, R. Shwathi, Compact fractalbased bandpass filter with high selectivity for terahertz applications. *Opt. Quant. Electron.* **55**, 960 (2023). <https://doi.org/10.1007/s11082-023-05269-8>
 15. H. Shahounvand, A. Fard, M.B. Tavakoli, Design, simulation and fabrication of a new terahertz cross-shaped metamaterial bandpass filter to obtain a narrow frequency bandwidth. *Opt. Quant. Electron.* **54**, 120 (2022). <https://doi.org/10.1007/s11082-021-03502-w>
 16. Z. Che, G. Zhang, P. Ren, J. Yue, Z. Li, Y. Lun, J. Suo, J. Zhu, Q. Zhang, Y. Feng, Narrow bandpass filter based on vanadium dioxide can be used for terahertz stealth. *J. Opt.* **51**, 336–342 (2022). <https://doi.org/10.1007/s12596-021-00764-1>
 17. J.X. Zhuang, W. Hong, Z.C. Hao, Design and analysis of a terahertz bandpass filter. In *IEEE International Wireless Symposium.* 1–4 (2015). <https://doi.org/10.1109/IEEE-IWS.2015.7164597>
 18. K. Sagadevan, D. Sathish Kumar, S. Rajagopalan, The design of split ring resonator (SRR) based terahertz bandpass filter and comparison of various types of filters. *J. Phys. Conf. Ser.* **1717**, 012052 (2021). <https://doi.org/10.1088/1742-6596/1717/1/012052>
 19. N. Zhang, R. Song, M. Hu, G. Shan, C. Wang, J. Yang, A low-loss design of bandpass filter at the terahertz band. *IEEE Microw. Wirel. Compon. Lett.* **28**(7), 573–575 (2018). <https://doi.org/10.1109/LMWC.2018.2835650>
 20. B.E. Caroline, K. Sagadevan, S.K. Danasegaran, S. Kumar, Characterization of a pentagonal CSRR bandpass filter for terahertz applications. *J. Electron. Mater.* **51**, 5405–5416 (2022). <https://doi.org/10.1007/s11664-022-09779-1>
 21. S. Yadollahzadeh, H. Baghban, Enhanced optical characteristics of terahertz bandpass filters based on plasmonic nanoparticles. *J. Nanophotonics.* **10**(2), 026002 (2016). <https://doi.org/10.1117/1.JNP.10.026002>
 22. A.B. Asl, A. Rostami, I.S. Amiri, Terahertz band pass filter design using multilayer metamaterials. *Opt. Quant. Electron.* **52**, 155 (2020). <https://doi.org/10.1007/s11082-020-02268-x>
 23. X. Ri-Hui, L. Jiu-Sheng, Double-Layer frequency selective surface for terahertz bandpass filter. *J. Infrared Milli Terahz Waves.* **39**, 1039–1046 (2018). <https://doi.org/10.1007/s10762-018-0527-x>
 24. G. Kaur, C. Jain, M. Rattan, Multiband Antenna Deploying Swastika Slotted Fractal for WLAN Utilities. In *IEEE India Council International Conference.* 1–5 (2017). <https://doi.org/10.1109/INDICON.2017.8487530>
 25. S. Ankit, C. Radhika, B. Sriya, S. Vidhi, N. Vikas, S. Deepanjan, *Swastika's Voyage: where It all Started* (Cygnus Advertising Pvt. Ltd, India, 2016)
 26. P. Nagaraju, I. Khan, H.V. Kumaraswamy, D.H. Sachina, K.R. Sudhindra, Analysis of SWASTIK-shaped slotted MSPA antenna for 5G sub band applications. In *International Conference on Intelligent Engineering Approach.* 80–85 (2022). <https://doi.org/10.1016/j.gltip.2022.04.018>
 27. A.D. Jaiswal, S.J. Vignesh, A. Mekap, D. Yadav, High-efficiency and high-gain swastik shape slotted microstrip planar antenna with suspended ground for 5G wireless applications. In *IEEE International Conference on Computing, Power and Communication Technologies.* 1–6 (2021). <https://doi.org/10.1109/GUCO50781.2021.9573562>
 28. B.B. Mandelbrot, *The Fractal Geometry of Nature* (W.H. Freeman, San Francisco, 1982)
 29. D. Sri Sai Satyanarayana, S.R. Koppula, S. Murki, Multi-layered swastika shape antenna patch design for GSM and WiMAX applications. In *IET Conference Proceedings on Smart Cities Symposium.* 282–285 (2021). <https://doi.org/10.1049/icep.2021.0964>
 30. S.M. Shamim, M.S. Uddin, M. Hasan, M. Samad, Design and implementation of miniaturized wideband microstrip patch antenna for high-speed terahertz applications. *J. Comput. Electron.* **20**, 604–610 (2021). <https://doi.org/10.1007/s10825-020-01587-2>
 31. M. Gezimati, G. Singh, Terahertz imaging and sensing for healthcare: current status and future perspectives. *IEEE Access.* **11**, 18590–18619 (2023). <https://doi.org/10.1109/ACCESS.2023.3247196>
 32. J.S. Hong, *Microstrip Filters for RF/Microwave Applications* (Wiley, New Jersey, 2011)

Publisher's note Springer Nature remains neutral with regard to jurisdictional claims in published maps and institutional affiliations.

Springer Nature or its licensor (e.g. a society or other partner) holds exclusive rights to this article under a publishing agreement with the author(s) or other rightsholder(s); author self-archiving of the accepted

manuscript version of this article is solely governed by the terms of such publishing agreement and applicable law.